

Study on ash deposition under oxyfuel combustion of coal/biomass blends

L. Fryda^{a,*}, C. Sobrino^b, M. Cieplik^a, W.L. van de Kamp^a



^aEnergy Research Centre of the Netherlands, Biomass, Coal and Environmental Research (ECN), The Netherlands

^bProcess and Energy Department, Faculty of Mechanical, Maritime and Materials Engineering, Delft University of Technology, The Netherlands

A B S T R A C T

Combustion in an O₂/CO₂ mixture (oxyfuel) has been recognized as a promising technology for CO₂ capture as it produces a high CO₂ concentration flue gas. Furthermore, biofuels in general contribute to CO₂ reduction in comparison with fossil fuels as they are considered CO₂ neutral. Ash formation and deposition (surface fouling) behavior of coal/biomass blends under O₂/CO₂ combustion conditions is still not extensively studied. Aim of this work is the comparative study of ash formation and deposition of selected coal/biomass blends under oxyfuel and air conditions in a lab scale pulverized coal combustor (drop tube). The fuels used were Russian and South African coals and their blends with Shea meal (cocoa). A horizontal deposition probe, equipped with thermocouples and heat transfer sensors for on line data acquisition, was placed at a fixed distance from the burner in order to simulate the ash deposition on heat transfer surfaces (e.g. water or steam tubes). Furthermore, a cascade impactor (staged filter) was used to obtain size distributed ash samples including the submicron range at the reactor exit. The deposition ratio and propensity measured for the various experimental conditions were higher in all oxyfuel cases. The SEM/EDS and ICP analyses of the deposit and cascade impactor ash samples indicate K interactions with the alumina silicates and to a smaller extend with Cl, which was all released in the gas phase, in both the oxyfuel and air combustion samples. Sulfur was depleted in both the air or oxyfuel ash deposits. S and K enrichment was detected in the fine ash stages, slightly increased under air combustion conditions. Chemical equilibrium calculations were carried out to facilitate the interpretation of the measured data; the results indicate that temperature dependence and fuels/blends ash composition are the major factors affecting gaseous compounds and ash composition rather than the combustion environment, which seems to affect the fine ash (submicron) ash composition, and the ash deposition mechanisms.

1. Introduction and scope of work

Combustion in O₂/CO₂ mixture (oxyfuel) has been recognized as a promising technology for CO₂ capture as it produces a high CO₂ concentration flue gas [1–7]. This technology consists of combusting the fuel in a mixture of oxygen, produced in an Air Separation Unit, and recirculated flue gas. Oxy fuel combustion and flue gas scrubbing (to separate the CO₂ from the combustion products using amines) are technologies that can be retrofitted to existing units. Including biomass co firing in the oxyfuel concept, helps achieving even negative net emissions, which will increase further the political and public support for CCS. Biomass co firing can address the technical CCS challenges with different percentages of biomass co fired, according to the Zero Emission Platform reports on the current status of the oxyfuel technology [8], however some technological blocks still need to be fully validated prior to pro-

ceeding with commercializing the technology. One of these technology blocks that need validation and further Research and Development is the oxyfuel combustion process itself, including fuel preparation and including biomass cofiring. At the same level lies the fuel recycling issue, including the level of gas cleaning necessary to allow for problem free boiler operation. The overall process integration, e.g. heat stream matching as well as advanced boiler materials for USC operation are also still subject to research and development, in order to validate the concept. In this frame, targeted lab scale tests are an easy and fast way to gather information and hints on how to proceed in the pilot scale. More experimental results in different lab scale installations are necessary to identify problems, if existing, and propose counteractions, and also try a wide variety of fuels and combustion conditions, parameters that are impossible to alter easily in the pilot and large scale.

An overview on research activities and technology developments on oxyfuel combustion including char combustion temperatures, fuel burnout, gas composition, heat transfer, coal reactivity and flame ignition has been recently published by Wall et al. [9]. The characteristics of combustion under O₂/CO₂ differ from air combustion in several aspects, e.g. gas composition, gas

* Corresponding author. Address: Energy Research Centre of the Netherlands (ECN), P.O. Box 1, 1755 ZG Petten, The Netherlands. Tel.: +31 224 564641; fax: +31 224 568487.

E-mail address: fryda@ecn.nl (L. Fryda).

Nomenclature

<i>DP</i>	deposition propensity (%)	<i>SEM/EDS</i>	scanning electron microscope/energy dispersive spectroscopy
<i>DR</i>	deposition ratio ()	$X_{dep,i}$	mass fraction of the element <i>i</i> (expressed as oxide)
<i>DTF</i>	drop tube furnace	$X_{ash,i}$	mass fraction of the element <i>i</i>
<i>EF</i>	enrichment factor	R_f	fouling factor ($K m^2/W$)
FACTSage®	facility for analysis of chemical thermodynamics		
ICP	inductively coupled plasma	<i>Subscripts</i>	
<i>LCS</i>	lab scale combustor simulator	<i>fa</i>	fly ash
<i>LHV</i>	fuel low heating value ($MJ kg^{-1}$ for solids/ $MJ m_n^{-1}$ for gases)	<i>g</i>	gas phase
m_{dep}	ash mass deposited (gr)	<i>s</i>	solid phase
m_{ash}	ash mass fed through the fuel (gr)	<i>slag</i>	slag phase
m_{fuel}	mass of fuel fed (gr)		

density, flow field. This different gas environment experienced by fuel particles might have an impact on the combustion processes including ignition, combustion characteristics, char reaction, and subsequently, ash and pollutants formation [10]. The consequence of this becomes important when the pulverized fuel boilers are planned to be retrofitted to oxyfuel. The effect of oxyfuel combustion on trace elements emissions and fly ash size distribution is uncertain, but it is expected that the behavior of minerals will be affected by the change in environment. For example, the high carbon dioxide partial pressures under oxyfuel will increase the decomposition temperature of carbonates [4]. Therefore in this introductory section an effort is made to gather the relevant literature on the parameters that are expected to affect the inorganic elements vaporization and ash deposition behavior in the combustor.

Ash particle formation under oxyfuel combustion has been addressed by Sheng et al. [10–12]. Specifically in [10], coal ash particles were collected at the bottom of a drop tube combustor using a low pressure impactor. It was found that O_2/CO_2 combustion decreased the size of the submicron mode center as well as the yield of the submicron particles compared to air combustion for the same oxygen concentrations. Increasing the oxygen concentration decreased the observed difference between the two combustion atmospheres. In [12], pulverized coals were fired in O_2/CO_2 and O_2/N_2 mixtures in a drop tube furnace. Qualitative XRD analysis showed that, in comparison to O_2/N_2 combustion, O_2/CO_2 combustion did not significantly change the main crystalline phases formed in residue ashes, implying no significant impacts on ash formation behaviors of the main coal minerals. Mössbauer spectroscopic analysis indicated that the variation between O_2/CO_2 and O_2/N_2 combustion did not affect the ash formation mechanisms of iron bearing minerals, but affected the relative percentages of iron species formed in the ashes. O_2/CO_2 combustion resulted in more iron melting into glass silicates in the ash. The differences observed in the ash formed under the two atmospheres were attributed to the impact of combustion gas atmosphere on coal char combustion temperatures, which influenced the ash formation behaviors of included minerals.

The experimental work of Suriyawong et al. [13] focused on ash formation under O_2/CO_2 combustion of a subbituminous coal in a drop tube furnace; it was observed that the mean size of submicron ash particles formed in O_2/CO_2 combustion was smaller than that formed in conventional air combustion. In [9] on the contrary, the size distribution and chemical composition of bulk fly ash did not differ significantly when produced in oxyfuel combustion and air combustion. The work described in [11], burning a high aluminum coal in a drop tube furnace to compare the ash formation in O_2/CO_2 combustion and air combustion, shows that O_2/CO_2 combustion did not significantly affect the transformations of main

minerals, but did affect the fine ash formation, consistent with the observations of Suriyawong et al. [13].

A significant proportion of the submicron ash generated during coal combustion is believed to be the result of mechanisms including the vaporization and homogeneous condensation processes of refractory oxides such as SiO_2 , CaO , MgO and Fe_2O_3 [12,14,15]. A number of studies focus on solid fuel/char burnout in O_2/CO_2 environments. Bejarano and Levendis [16] conducted a fundamental investigation on the combustion of single particles of coal in O_2/N_2 and O_2/CO_2 environments. They observed increasing particle temperatures and decreasing burnout times for increasing oxygen fractions, being the particle temperature higher and the burnout time lower for the O_2/N_2 environment at the same oxygen molar fraction. They reported equivalent bituminous coal volatile and char temperatures to those measured in air when the oxygen content in the O_2/CO_2 mixture was ~30%, whereas this concentration had to be 30–35% to attain similar burnout times. In [17] the combustion rates of two pulverized coal chars were measured in both conventional and oxygen enriched atmospheres. Predicted char particle temperatures tended to be low for combustion in oxygen depleted environments. In [11] the impact on mineral transformation and fine ash formation of O_2/CO_2 combustion of a high aluminum ash coal was studied. The main conclusion here as well was that O_2/CO_2 combustion had an impact on the local char particle combustion temperature and consequently on the ash vaporization and the ash mineral composition. The varying bulk gas composition (e.g., CO_2 concentration) changed the CO/CO_2 ratio within the burning char particle affecting the vaporization of refractory oxides, as observed by Krishnamoorthy and Veranth [18], who modeled the combustion of a single char particle. As a consequence, this affects accordingly the chemical composition of fine ash particles. The varying char combustion temperatures and locally reducing conditions might reduce minerals to more volatile forms. Char temperature fluctuations between air and oxyfuel combustion, affect therefore the degree of release of the included minerals and alter their extent of vaporization. Reducing conditions may also have a notable impact on excluded minerals, particularly iron based minerals [19].

Zheng and Furimsky [20] carried out chemical equilibrium calculations using the software FACTSage® to study the effect of CO_2 on the emissions and the ash composition under coal combustion. They concluded that the combustion medium had little effect on the ash chemical composition, but they did not exclude the effect of the carbonation and/or sulfation reactions of basic components on ash composition for the coals containing a high alkaline mineral matter. However it was not stated if molten ash phases are included as possible products in the calculations. Zhao et al. [21] applied the same approach to study the evaporation of mineral elements in O_2/CO_2 combustion. For temperatures lower than

2000 K they did not find differences between the combustion in air and O_2/CO_2 .

Although significant work exists studying the interactions of S/K/Cl and their significance in fine ash and aerosol formation, explaining in detail the possible mechanisms that lead to the main ash elemental composition of fine ash and aerosols, e.g. [22,23], so far little work is reported on the possible effect of oxyfuel combustion conditions on the elemental composition as well as the fine ash yield in comparison to conventional air firing.

Considering biomass cofired with coal under oxyfuel conditions, there is only one published work to our knowledge. Tests in an entrained flow reactor to study the ignition and burnout of coals and blends with biomass under oxyfuel and air (reference) conditions by Arias et al. [24], showed worsening of the ignition temperature in CO_2/O_2 mixtures when the oxygen concentration was the same as that of the air; however at oxygen concentrations of 30% or higher, an improvement in ignition was observed. The results of this work indicate that coal burnout can be improved by blending biomass in CO_2/O_2 mixtures.

The integration of biomass in the oxyfuel co firing blend has not yet been studied extensively and there are open questions prior to utilising biomass under oxyfuel conditions, as for example, the ignition of blends under oxyfuel conditions, proper temperature conditions, the degree of flue gas cleaning prior to recirculation, the effect of biomass ash components under CO_2 and increased O_2 conditions or the behavior of ash deposition under varying gaseous environment. The flue gas enrichment in S and Cl due to the necessary recirculation can affect the ash formation and deposition, inducing further ash melting and enhancing the fine ash particle formation [23].

The aim of this work is the comparative study of ash formation and deposition of selected coal/biomass blends under oxyfuel and air conditions in a lab scale pulverized coal combustor. The fuels used were Russian and South African coals and their 20% w/w blends with Shea meal (cocoa). Ash samples were subjected to SEM/EDS and ICP analyses and chemical equilibrium calculations using FACTSage[®] were carried out to facilitate the interpretation of the measured data.

2. Description of experimental facility and test procedure

The most prominent example of a lab scale installation for dynamic fuel characterisation is a so called drop tube furnace. In its basic form, the installation constitutes of a vertical reactor, which is externally heated, mostly by an electric furnace. Installations of such general layout, have been utilised by many EU research institutes. A few, to name EMC/Casella/RWE N Power (UK), INCAR (SP) or CERCHAR (F) and ECN (NL) attempted even a harmonisation of the research techniques utilising the DTF in the frame of the EU Research Fund for Coal and Steel project ECSC 7220 PR 106. The main advantage of the lab scale DTF is its simplicity and flexibility in creating virtually any combustion environment and studying dynamically fuel conversion and ash formation. A classical DTF however, knows also certain limitations. For example, the heating rates of a fuel particle falling freely in a heated tube are still at least one order of magnitude slower than in a real combustion system, where fuel particles are instantaneously subjected upon injection to the scouring heat of the pulverized fuel flame. Many of the said limitations can be overcome with specific design features. A good example of such advanced DTF is Lab scale Combustion Simulator, developed and optimised in the past decade by ECN. The ECN lab scale combustion simulator (LCS) shown in Fig. 1, consists of an extensively modified drop tube furnace, equipped with a flat flame, multi stage, premixed gas burner, into which the investigated solid pulverized fuel is injected. This provides adequate heating rates (10^5 K/s), well in range with full scale PF boilers. The reactor is equipped with a conical inlet, which causes the flue gas and char/ash particles to decelerate, enabling for long residence times in spite of a relative short length. The char particles are then lead into an electrically heated reactor tube, where they are further combusted. The staged gas burner accommodates high initial heating rates and temperatures and provides the possibility to simulate air staging as in low NO_x burners and also the presence of specific combustion products such as, e.g., SO_2 . The furnace has ~ 1 m length. The burner consists of two concentric sub burners viz. a primary, inner burner (10.9 mm ID) and a secondary, outer burner (60.7 mm

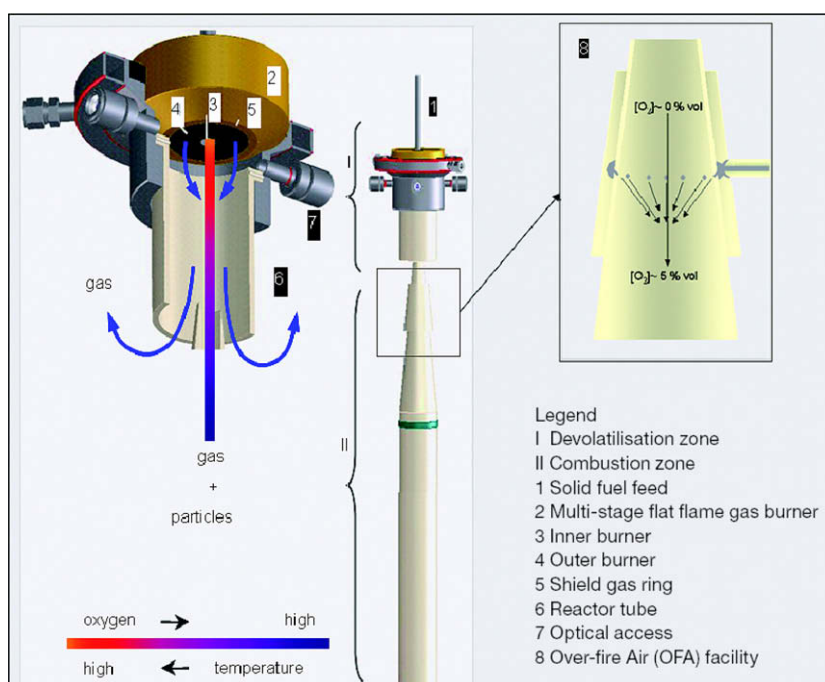


Fig. 1. Schematic of the ECN Lab-scale Combustion Simulator (LCS).

ID). The inner burner is supplied with a mixture of O_2 , CH_4 , and CO_2 or N_2 with an oxygen lean rate. In the outer burner the gaseous mixture of O_2 , CH_4 , and CO_2 or N_2 provides the necessary oxygen in order to complete the combustion. Fuel particles are fed through the inner burner and are rapidly heated ($>10^5$ °C/s) to the high temperature level of, e.g., a coal flame (1400–1600 °C). Typically, low particle feed rates of 1.5 g/h are used in order to control the gaseous environment of each particle by means of the imposed gas burner conditions. This implies that heating and devolatilisation of the fuel particles takes place in an oxygen deficient zone (indicated as I in Fig. 1) provided by the primary, inner burner, whereas subsequent char combustion takes place in a zone with excess oxygen (indicated as II in Fig. 1). The transition from oxygen lean to oxygen rich takes place and is completed in zone I by diffusion. The resulting gas/particle flow is then drawn into a 76 mm ID alumina reactor tube for complete oxidation of the fuel. From a distance of ~ 130 mm from the burner the tube is surrounded by two 3.4 kW furnace sections equipped with Kanthal Super 1800 elements with a maximum element temperature of 1700 °C. The temperature of each zone is independently controlled by a Eurotherm controller and two S type thermocouples, at 1450 °C. The furnace temperature profile (Fig. 2a) was measured in the absence of the particles, using S type thermocouples. The flue gas composition is continuously monitored using a UV analyzer for NO and NO_2 , a NDIR for CO and CO_2 and a magneto mechanical analyzer for O_2 .

The residence times are also shown in Fig. 2b, both in the flame area close to the burner plate as well as along the reactor. Resi-

dence time calculations are based on the volume flows, the gas velocity, assuming laminar flow and taking into account the reactor geometry, axial gas temperature profile and the particle terminal velocity. We matched the volume flow rates in all cases, in both the inner and the outer burner, in order to have the same or very close volume flows. The selection of flows was such as to allow for the same residence times in all experiments for the given temperature profiles. A suction pump that operates at a constant volume flow rate also assures for homogeneous velocities and therefore isokinetic conditions in the reactor. The small difference in residence times in the burner area is due to the fact that flows were slightly adjusted in order to match the temperature profiles between air and oxyfuel combustion. Boiler tube fouling studies can be carried out using a horizontal probe placed at ~ 850 mm from the burner. This probe simulates the gas/particles flow around a single boiler tube in the convective section of a boiler. It is provided with a ring shaped heat flux sensor installed on the horizontal tube as well as with a detachable tubular deposition substrate. The surface temperature of the probe is controlled by the air cooling system and maintained at 660 °C. It is supported that boiler retrofit to oxyfuel operation should be applied to modern and high efficient power plants, rather than to older and less efficient power plant units, in order to better amortize the large efficiency penalty after applying CCS measures. In that case the steam conditions are expected to be higher than in the older power stations. The surface temperature of the probe was chosen in order to include supercritical steam conditions, which is an option for oxyfuel applications. The effect of the surface temperature of the

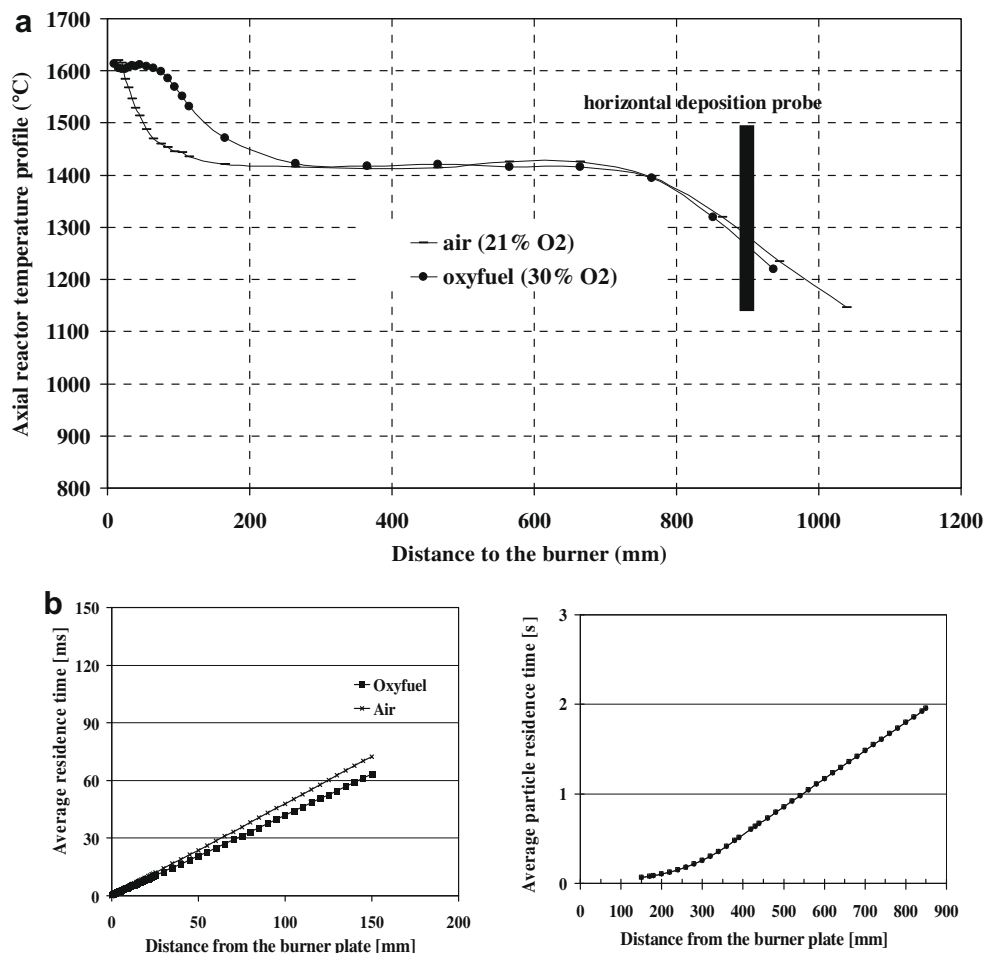


Fig. 2. (a) LCS temperature profiles under air and oxyfuel conditions and (b) LCS residence times under air and oxyfuel conditions.

probe was not further studied in this paper and should be taken into consideration in future works.

Deposition samples can be collected in either the sensor area (sample No. 1) or the detachable probe surface (sample No. 2). When the sensor is used, on line data on the influence of the deposit on the effective heat flux through the tube wall are collected allowing calculating the fouling factor, which is defined as the inverse of the overall heat transfer coefficient. The ash collected on the sensor was subjected to ICP/AES analysis. It is also possible to collect ash on a detachable substrate and then fix the sample with epoxy for further SEM/EDS analysis. The remaining particles not deposited on the horizontal probe are collected by a vertically adjustable cooled probe at the end of the drop tube reactor on a porous filter (sample No. 3), which is further submitted to ICP analysis, together with sample No. 1 from the horizontal ash deposition probe. The carbon in ash was also determined for all ash samples. The particle size distribution and the density of the ash samples collected in the horizontal probe and the filter were also determined. As it is a dilute system in terms of solids/gas ratio, compared with an autothermal full scale PF furnace, the large volume of the surrounding flue gas kept at a constant temperature helps to maintain a relevant temperature on the surface of the char/ash particles, until the moment these reach a cooled surface of the deposition probe, avoiding inhomogeneous or too high peak temperatures in the char particles.

Deposition tests were carried out with two coals (Russian and South African) and their blends with Shea meal (cocoa residues) at 20 wt.% combusted in O₂/CO₂, with a 30 vol.% of oxygen in order to achieve the same adiabatic flame temperature and similar heat transfer characteristics than in air combustion. Proximate (ash, VM and moisture % (w/w) oven/gravimetry) and ultimate analyses (C, H, N, O, S Carlo Erba analyzer), as well as inorganic elemental

composition using ICP/AES (29 elements in total) were performed on the fuels, the results shown in Table 1. The fuels were all ground to less than 500 μm: 250 μm < d_p < 500 μm in order to be fed in the brush feeder. A series of combustion tests with Russian and South African coals and blends in air (79 vol.% N₂ and 21 vol.% O₂) were carried out as reference as well. In all oxyfuel condition test runs, in order to simulate flue gas recycling that will possibly contain, at least in traces, sulfur in the form of SO_x, a small volume flow of H₂S was added together with the fuel, which is oxidised immediately to SO₂/SO₃. It is still argued on the level of gas cleaning that has to be applied in the oxyfuel combustion; therefore defining the effect of a sulfur surplus on the deposition behavior was considered important at this stage. Water vapor was not included in our tests, as part of the simulated recycled gas input, simulating dry recycling. Moisture in the recycled flue gas would increase the heat transfer coefficient of the flue gases even further, and this would possibly lead to a slightly lower recycling ratio in comparison with a dry recycling system, and a lower CO₂ concentration on the recycled flue gas. In the other referenced works there was no indication that steam vapor was added to the O₂ & CO₂ stream either. In any case, gas cleaning prior to recycling implies that the gas is cooled down considerably in order to pass through the various gas cleaning devices. Finally, two tests (Russian coal in O₂/N₂ and in O₂/CO₂) were run using a cascade impactor (Pilat Mark) in order to obtain size distributed ash samples and obtain insight into fine ash formation and composition under varying combustion environments (air and oxyfuel). Seven fractions in the size range >50 μm down to ~0.3 μm were obtained. Nucleo pore polycarbonate filters were placed in the stage plates to allow subsequent microscopic analysis.

3. Results and discussion

3.1. Visual inspection data

In general, the ash deposited on the sensor and on the deposit substrate was loose and powdery and with the slightest movement the ash sample would fall off or diffuse in the air. In terms of color and appearance the deposits did not vary between oxyfuel and air combustion. The deposit thickness difference however was notable amongst air and oxyfuel trials, the oxyfuel deposits being thicker. A thin white layer could be seen on the sides and bottom of some of the probes, possibly alkali chloride salts condensed onto the cool probe surface during the initial stages of deposit formation.

3.2. Ash deposition rates and deposition propensity

All ash samples collected in the horizontal probe during the deposition experiments as well as the filter ash samples were weighed. Several parameters have been introduced in order to assess the deposition tendency. First, the ash deposition ratio *DR* is calculated, which is defined as the ratio of the ash collected on the probe, *m_{dep}*, to the fuel fed, *m_{fuel}*, both quantities measured directly

$$DR = \frac{m_{dep}}{m_{fuel}} \quad (1)$$

Second, in order to normalize the ash deposition in relation with the fuel ash content, the deposition propensity *DP* is introduced, defined as the percentage of the ash collected on the deposit probe *m_{dep}* to the ash content in the fuel fed, *m_{ash}*. This ash content in the fuel is given by the proximate analysis of the fuel. The deposition propensity, here expressed in %, provides more insight into

Table 1
Chemical analysis of the used fuels.

Fuel	Russian coal	Shea meal	South African
Moisture/Std Dev	3.4/0.5	11.1/1.4	3.9/0.3
<i>Proximate analysis (% mass, dry fuel basis)</i>			
Ash @ 815 °C/Std Dev (of sample)	14.9/0.5	5.4/0.2	12.8/0.2
Volatile matter/Std Dev	29.0/1.1	61.9/1.3	25.3/0.3
HHV (kJ/kg)/Std Dev	27800 / 200	19410/80	28225/60
Initial deformation (°C)	1250	1140	1350
Hemisphere temperature (°C)	1360	1310	1375
Flow temperature (°C)	1410	1330	1400
<i>Ultimate analysis (% mass, dry fuel basis)</i>			
C/Std Dev	68/2	49.4/0.8	70/3
H/Std Dev	4.0/0.3	5.35/0.05	3.8/0.3
N/Std Dev	0.87/0.12	2.61/0.04	1.34/0.07
S/Std Dev	0.35/0.02	0.27/0.01	0.53/0.02
O by diff.	11.6	40.1	9.2
<i>Ash composition (mg/kg fuel, dry basis)</i>			
Na (±7) ^a	405	179	269
Mg (±1)	1277	1937	1665
Al (±4)	16583	772	19794
Si (±90)	34841	1861	21931
P (±15)	386	1684	750
K (±20)	2390	20790	790
Ca (±20)	2750	2140	7500
Ti (±8)	622	47	843
Mn (±6)	89	24	52
Fe (±4)	6077	1095	2907
Zn (±1)	21	4	10
Pb (±20)	10	0	0
Sr (±5)	183	18	454
Ba (±5)	260	22	349
B (±1)	43	19	41
Cl (±20)	100	800	50

^a Equipment error.

the inherent deposition characteristics of the different fuels, as it accounts for variations in fuel ash content

$$DP = \frac{m_{dep}}{m_{ash}} (\%) \quad (2)$$

Fig. 3 shows the deposition ratio and the deposition propensity as defined for the various test runs.

As mentioned, the system is dilute in terms of solids/gas ratio. The flame temperature is controlled by the flat flame gas burner, and the temperature profile in the reactor is controlled by external heaters. The main flue gas flow and composition are formed and controlled by the methane and oxidant streams introduced by the staged burner. The low particle feed rates are used in order to control the gaseous environment of each particle by means of the imposed gas burner conditions. Therefore the influence of a 20% replacement of the solid fuel (coal) by biomass, on the total heat release and oxygen demand is insignificant.

The ash content of the fuels and blends, included in the results evaluation and presentation, is shown in Table 1, applying the standard ash characterisation methods. It can be seen that the deposition ratio (Fig. 3) is, as expected, increasing with the ash content of the fuels, and it can be observed that the deposition ratios are lower under air combustion. The two coals studied present in general lower deposition propensities when they are blended with cocoa, probably due to ash elements interactions, e.g. Cl present in the biomass forming compounds that enter the gas phase.

A large number of further oxyfuel vs. air tests were conducted recently in our facility, using different fuels blends than the presented in this work, showing the same tendency. The ash collected in the deposition probes for the different experiments were always easy to detach from the probe being a loose powder. The carbon in ash in the samples was measured, confirming that the higher deposition of the oxyfuel samples was not due to unburnt fuel particles that might be present in the deposits. Carbon in ash values are shown in Table 2, where it can be seen that there is on average a somewhat higher carbon percentage in the air case ash, but despite that, neither the measured ash deposited nor the fouling factors were increased in the air case compared to the oxyfuel case. Fur

Table 2
Carbon in ash and flue gas composition for the test cases.

Fuel blend	C in ash (w/w %, dry)	Flue gas at the exit (CO ₂ %, O ₂ %, CO ppm)
Russian coal (air)	1.75	10%/3.0%/14 ppm
Russian coal (oxyfuel)	2.57	87%/2.5%/22 ppm
Russian coal/cocoa (air)	7.6	9.5%/2.5%/16 ppm
Russian coal/cocoa (oxyfuel)	2.17	86%/3.0%/25 ppm
South African coal (air)	6.7	9.5%/2.8%/20 ppm
South African coal (oxyfuel)	10.1	83%/2.8%/30 ppm
South African coal /cocoa (air)	6.8	9.5%/3.0%/15 ppm
South African coal/cocoa (oxyfuel)	2.73	85%/2.8%/21 ppm
Russian Coal (air) Cascade Impactor	Not detected	10%/3.3%/4 ppm
Russian Coal (oxyfuel) Cascade Impactor	Not detected	83%/3.6%/0 ppm

thermore, during the tests we also monitored the CO₂ and O₂ levels in the reactor exit together with the flue gas composition. The CO levels were always low, slightly higher than the levels of CO emissions when the reactor operated on the methane (pilot) flame without fuel, indicating satisfactory combustion, not loading the deposited ash with high loads of carbon particles.

A final issue possibly affecting ash deposition behavior is the flame temperature profiles in the two combustion conditions; it can be observed that although the tip flame temperature is approximately the same under oxyfuel and air conditions, the flame length is somewhat larger in the oxyfuel case, as implied by the higher temperatures, and therefore the particles are exposed to higher temperatures during a longer time. Variations in exposition times or peak flame temperatures might indeed lead to variations in 'sticky' mineral matter amounts which are likely to agglomerate, producing ash particles that are coarser and more prone to deposition. In our tests indeed, some of the particles' rounded shape observed in the microscope for both the oxyfuel and air samples, indicates that the ash was exposed to temperatures reaching the theoretical melting temperature of some of the ash compounds. However we did not observe slag in the sensor and deposit samples

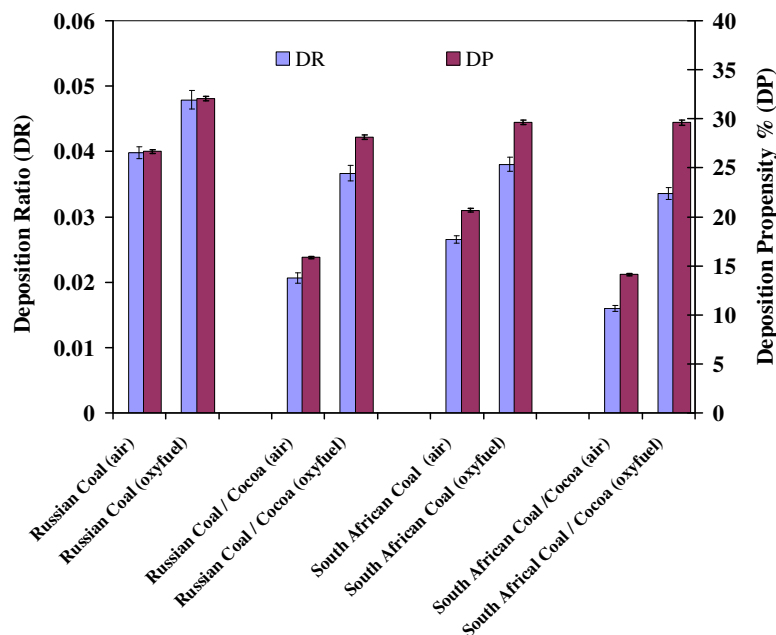


Fig. 3. Deposition ratio and deposition propensity for the fuels and blends combusted in air and O₂/CO₂.

when extracting the probe from the reactor, which would imply fluxing ash melt, as the material was powdery and easy to blow off.

An explanation of the observed differences in the ash deposition propensities is attempted considering the deposition mechanisms: inertial impaction including impaction and sticking, thermophoresis, condensation and chemical reaction [25]. Inertial impaction is prevailing in reactors as the present one, dependent on the variations in the physical gas properties, as e.g. the gas density of CO₂/O₂ mixture, which is higher than under N₂/O₂ conditions. This may explain the higher deposition ratios under oxyfuel firing. An other remark concerning inertial impaction in our reactor is that the deposits were found predominantly on the front side of the tube, as the deposition probe is placed in cross flow, promoting the collision of the particles in the front area. In addition, there was no deposition built up on the sides of the probe or even less on the down stream side of the probe, except of a thin layer of fine ash at the sides. This verifies the absence of ash slag and the presence of possibly other ash deposition mechanisms on our sampling rig, less dominant than inertial impaction, e.g. thermophoresis. A thin film formed by the alkalis condensing on the surface might have aided the formation of a first ash particle layer upon which the deposit started growing due to inertial impaction.

At this point though it must be mentioned that the effect of increased CO₂ partial pressure on carbonates formation (CaCO₃, FeCO₃), which might give a hint on the deposition behavior observed was not studied. This issue will be taken into account in the following research activities.

Therefore, we conclude that the systematic differences in the deposition behavior of the same blends under the two combustion conditions is due to the differences in the flow fields and in the physical properties (density, viscosity) of the gaseous mixtures.

The filter (fly) ash, collected at the reactor exit, preventing the analytical instruments, is the residual ash not captured in the deposition probe surface. Based on the ash mass balance, Fig. 4a shows the deposition ratio of the filter ash, using the same definition as for the deposit ash sample:

$$DR_{\text{filter ash}} = \frac{m_{\text{filter}}}{m_{\text{fuel}}} \quad (3)$$

which is the ratio of the ash collected in the filter m_{filter} , to the fuel fed m_{fuel} . In order to directly compare the distribution between the deposited ash and the ash collected in the filter for the two combustion environments, these two quantities are expressed as percent ages of the total ash fed, shown in Fig. 4b which shows the ash distribution percentages under air and oxyfuel conditions, between the deposited and filter ash in relation to the total fuel ash. The ash balance did not add up to 100%, but it was in all cases somewhat lower, around 90%.

Given the fact that the fuel mass flow rate, the quantities fed and the fuel particle size distribution are the same under air and oxyfuel conditions, together with the information on deposition ratio and propensity shown in Fig. 3, we can conclude that the ash deposition behaves differently between air and oxyfuel combustion. Less amount of ash deposited for the air case is observed together with a higher amount of fly ash found back in the filter, in comparison with the oxyfuel conditions.

Transferring the deposition behavior observations into the full scale is not straightforward, however. The LCS is a down fired entrained flow drop tube like test rig, in which all the particles, independent of the size and composition will end up at the bottom, where the sampling train is located, and in the filter ash. In a full scale power plant, opposed, tangentially or down fired, the prevailing deposition mechanisms are more complicated, affecting the ash distribution. However, the conclusion that under oxyfuel conditions systematically less fine ash was found back in the filter (fly ash) and more coarse ash was deposited, as opposed to the air

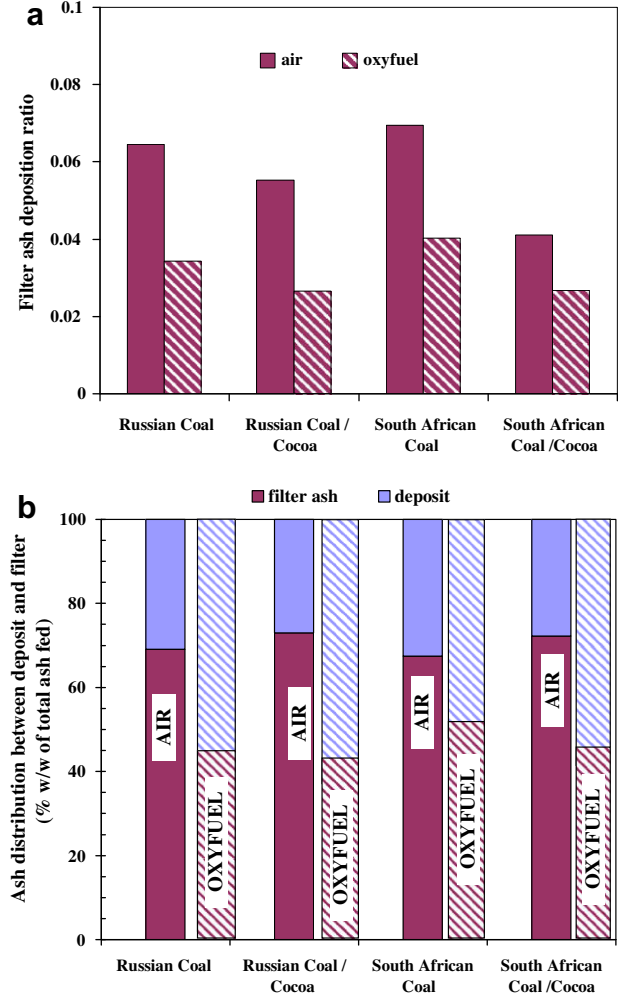


Fig. 4. (a) Filter ash deposition ratio and (b) ash distribution between deposit and filter ash for the fuels and blends combusted in air and O₂/CO₂.

case, can prove useful in the design of the heat exchanger tubes and surfaces generally, preventing excessive fouling in points that were not considered under conventional air operation.

3.3. Fouling factor calculation

Based on the heat flux data measured on line by the sensor probes the fouling factor R_f of the obtained deposits can be estimated, which corresponds to the ash deposits heat transfer resistance:

$$R_f = \left(\frac{1}{U_1} - \frac{1}{U_0} \right) \frac{T_g - T_c^1}{HF_1} - \frac{T_g - T_c^0}{HF_0} \quad (4)$$

where R_f fouling factor, (K m²)/W (heat transfer resistance); U_1 ash deposits heat transfer coefficient after time $t = t_1$, W/(K m²); U_0 initial heat transfer coefficient after $t = t_0 = 0$, W/(K m²); T_g flue gas temperature, K; T_c coolant medium temperature inside the deposition probe, K; HF_1 heat flux to the sensor after time $t = t_1$, W/m²; HF_0 initial heat flux to the sensor $t = t_0 = 0$, W/m².

The fouling factors are depicted in Fig. 5 as an almost linear function of the cumulative ash feed rate. The slopes of the curves plotted become independent of the fuels' various ash contents. The point at which fuel feeding started was taken as the beginning of the heat flux measurement. In all cases the heat flux, surface temperatures, cooling air flow rate and furnace temperatures reached steady state by the start of the deposition measurement.

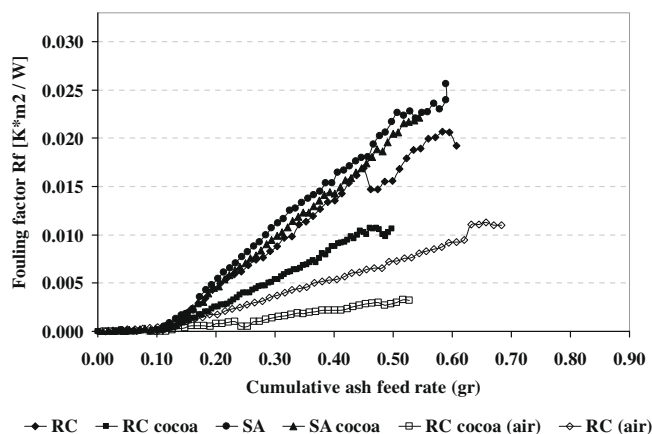


Fig. 5. Calculated fouling factors versus accumulated feed rate for the tested blends under air and oxyfuel conditions. RC = Russian coal, SA = South African coal.

The coal/cocoa blends show lower fouling factors than the coals, in accordance with the deposition propensity results. However, it has to be noted that generally a higher deposition propensity does not always imply that the fuel has a higher fouling propensity; other factors like the thermal conductivity of the deposition layer or the scattering of the deposit on the probe or the deposit density, might also play a role in the heat transfer properties of the deposition layer, affecting therefore the fouling factor value. The density of the deposit of filter ash samples was not measured in this testing series.

3.4. Chemical composition analysis: element enrichment ICP analyses of deposited and fly ash

The elemental enrichment was defined and quantified by performing a mass balance including the weights and inorganic compositions of the fuels and ash samples obtained from (1) the deposited ash, which resembles the bulk ash and (2) the fly ash, obtained from the filter, which contains the ash that was not deposited on the probe.

The results of the elemental composition of the deposited and filter ash are presented using the enrichment factor EF which describes the relative enrichment of an element in the sampled ash relative to its concentration in the fuel ash. The enrichment factor EF is defined for either the deposited ash or the filter ash as

$$EF_i = \frac{X_{dep,i}}{X_{ash,i}} \quad (5)$$

where $X_{dep,i}$ is the mass fraction of the element i (expressed as oxide) in either the deposit or the filter ash and $X_{ash,i}$ is the mass fraction of the element i (expressed as oxide) in the initial ash of the fuel prior to combustion. The results are given in Fig. 6a and b.

It can be observed that for the coal/cocoa blends the ash collected from the deposit probe is slightly depleted in potassium, as observed by other investigators [26]. This indicates that potassium enters the gas phase either due to Cl presence which is increased in the case of the Cl rich cocoa blends, facilitating the volatilization of elements that would otherwise deposit [27] or simply due to the fact that K in the biomass ash is more reactive, and therefore mobile, compared to coal ash K. In that case the slight decrease in EF is just due to the biomass addition, not implying biomass coal ash interactions. This could in any case explain the relatively lower deposition propensity of the coal/cocoa blends. However, the filter ash does not seem in all cases depleted in K, as observed for the Russian coal/cocoa blends, which is in agreement with other published works, e.g. [28], where the

increased Cl input is observed to lead to an increased K concentration in the fly ash, as it mobilizes the K, forming KCl which ends up either in the fly ash or on the cold surfaces. The released KCl can also condense on cold surfaces after the filter, as for example in our facility, on the glass capillary part of the membrane pump used for the gas sample into the gas analysis device, where a white film was observed after the blends experiments. Due to the very small sodium concentration in the fuel ash it is not safe to draw conclusions on its behavior.

All the deposit samples show almost complete chlorine depletion, as also reported in other works [29]. This indicates that Cl is released in the gas phase probably as HCl (and to a smaller degree as KCl) which might be found back in the fine ash (filter ash sample) or just pass through the filter without condensing. An exception is observed though in the fly ash samples of the Russian coal but in general Cl was detected in very low concentrations implying its volatilization. Another published work [22] also reported that NaCl and KCl become unstable and are not found in deposits at temperatures higher than 650 °C.

Also S is depleted in both the deposit as well as the filter ash, as it is suggested to react with alkalis and therefore enters the gas phase [19]. Under high temperatures and oxidising conditions, essentially all of the sulfur containing inorganic species in coal (primarily sulfates and pyrites) decompose to form SO_2 therefore none of the fuel sulfur passes unreacted through the combustor [27]. At the deposition probe temperature at 660 °C, some of the gaseous SO_2 reacts with alkaline earth and, to a lesser extent, alkali oxides and salts to form sulfates. Cocoa introduces some amount of Ca which could react with S into $CaSO_4$, which is a solid phase and also prone to deposit. This might explain the slightly higher S enrichment of the deposited ash of the coal/cocoa blends, but this is not observed for the filter ash of the Russian coal/cocoa blend. However, the relatively small sulfur concentration and the high Si/Al content of the fuels ash leads to the conclusion that, most of the potassium and sodium in the deposit is expected to form alkali aluminum silicates rather than bind with S. Alkalis also enter the gas phase due to the highly mobile Cl presence. The increase of enrichment of S and at some points of Cl in the fly ash, in comparison with the deposited ash, can be explained by considering condensation of gaseous phase elements on the finer fly ash which is caught by the filter. Such a conclusion however cannot be extracted for the alkalis, which show a relatively constant EF between deposited and filter (finer) ash.

Phosphorus EF values are similar for the various fuels' and blends' ashes and combustion conditions, with values slightly lower than 1. The other elements (Si, Al, Fe, Ca, Mg) show an $EF \sim 1$.

A major conclusion here is that a clear effect of the combustion environment, air vs. oxyfuel, on the EF results is not observed for the Russian coal and its blend. For the South African coal and its blend the EF of K is slightly higher for the air case, but since this is not the case for the whole range of the Russian coal tests, further work is needed in order to draw final conclusions.

As for the other elements (Si, Al, Fe, Ca, Mg), the EF is constant in all cases; therefore neither the combustion conditions nor the blends seem to affect the deposited or the filter ash enrichment.

3.5. Chemical composition analysis: element enrichment ICP analyses of sized distributed ash samples

Size distributed ash samples using a cascade impactor (staged filter) were collected during the combustion of Russian coal in air and O_2/CO_2 . The ash samples collected in the different stages of the impactor were weighed, subjected to ash composition analysis and observed with scanning electron microscopy (SEM/EDS). An effort is made in this section to obtain further insight into the effect of the combustion conditions, air and oxyfuel, on the release of ele

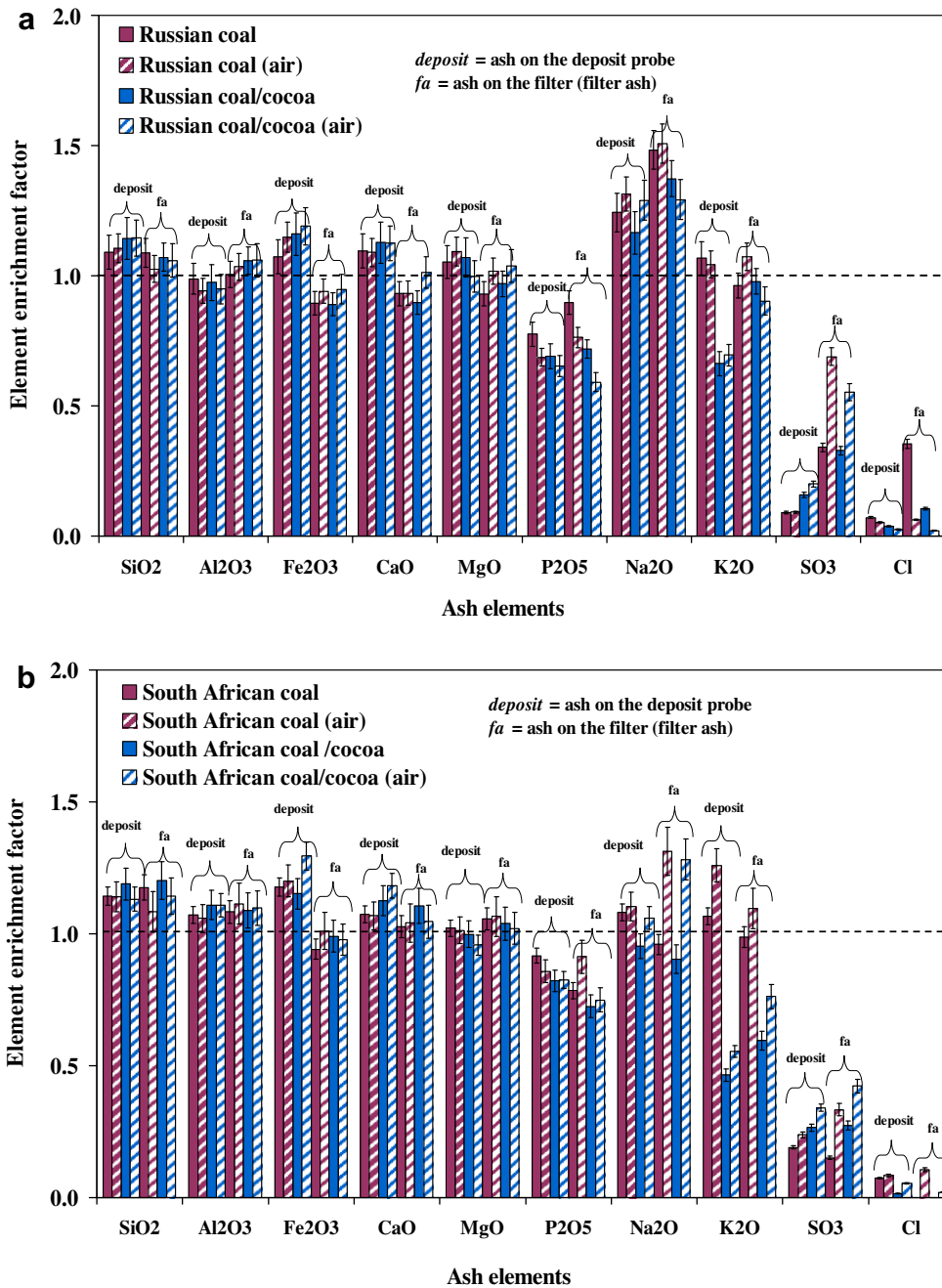


Fig. 6. (a) Element enrichment in the sensor (deposit) and filter ash for the Russian coal blends in air and oxyfuel and (b) Element enrichment in the sensor (deposit) and filter ash for the South African coal blends in air and oxyfuel.

ments in the fine ash and a comparison and evaluation of the observed results with results reported in the literature is attempted.

The enrichment factors EF of the main volatile elements in each stage, expressed as oxides, is shown in Fig. 7a and b. The advantage of the ICP ash analysis is the chlorine and carbon in ash detection, which is not possible to be detected in the SEM/EDS, however for very small quantities of ash, as in the fine ash stages (bottom stage) the SEM/EDS is more accurate. Therefore the results have been evaluated carefully taking into account all analyses.

It is observed that the concentration of the volatile elements in the finer ash stages is increased in relation to their percentage in the larger particle size area, in both air and oxyfuel conditions. This could be explained assuming vaporization and subsequent condensation of volatile elements (Na, K, S, Cl) on the fine ash particles, as

also observed and reported in other publications [23,19]. In [30] it is stated that the size dependent chemical composition of the sub micron ash indicates that the condensation of evaporated species was responsible for the formation of ash particles smaller than 0.3 μm . The lower concentrations in refractory oxides are due to a limited vaporization rate of these elements (including SiO_2 , Fe_2O_3 , CaO).

Even if only a small fraction of alkalis, Cl and S of the initial fuel ash is found in the gaseous phase, it is sufficient to produce a certain amount of submicron particles of which the inorganic (elemental) composition is quite different from the bulk fuel ash composition. This is due to the different ash formation mechanisms that determine the submicron ash formation, which is mainly condensation and nucleation of volatilized ash elements,

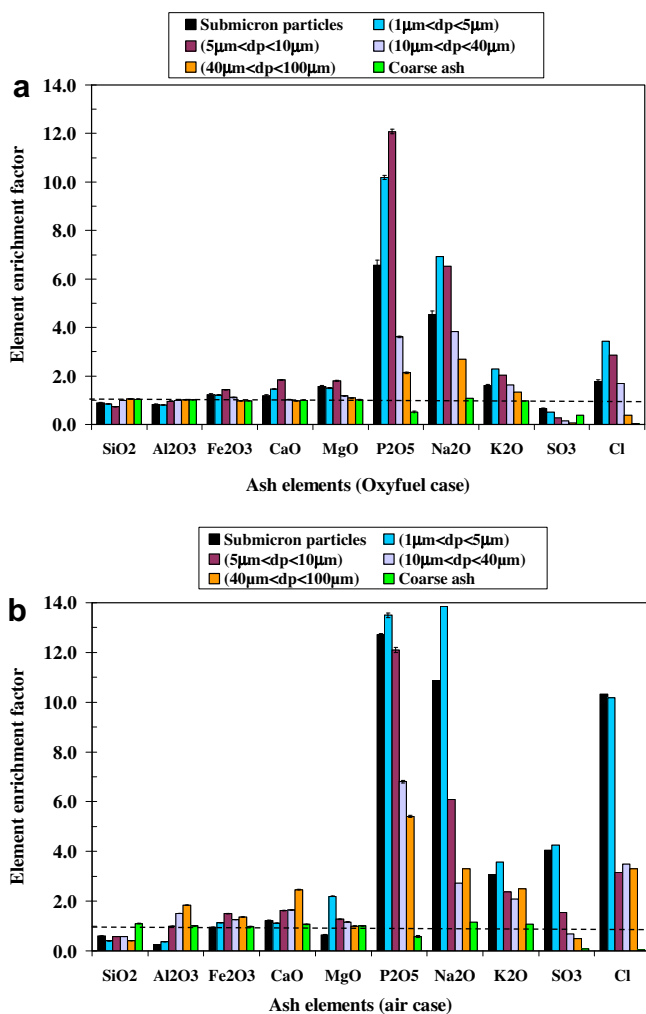


Fig. 7. (a) Element enrichment in the fine ash under oxyfuel conditions and (b) element enrichment in the fine ash under air conditions. Fuel: Russian coal.

as opposed to fragmentation of original mineral inclusions that define the formation of larger ash particles. Therefore the enrichment in S and K in the submicron ash does not seem in accordance with the tendency shown in Fig. 6, that shows EF values around 1 or less (depletion), however the submicron ash particles constitute a small fraction of the total ash produced and therefore do not change considerably the bulk ash composition.

Observing Fig. 7, the EF values for the coarse particles converge to the values shown in Fig. 6a and b. The differences in the EF values are diminished above a certain particle size for both combustion conditions, as the mechanism of ash formation for larger ash particles is not due to nucleation and condensation anymore, but as mentioned before, mainly to fragmentation. A change in the fine ash chemical composition between air and oxyfuel combustion can be observed, despite the fact that the bulk ash compositions do not show significant differences in the two cases.

In detail, observing the EF values, we can see that the oxyfuel ashes are more enriched in refractory elements (Ca, Si, Fe, Al, Mg, P) than the fine ash in the air case, which in turn is comparatively enriched in the more volatile elements like K, Na, S and even Cl. Therefore it could be concluded that the variation in the combustion conditions affect the release and initial vaporization of volatiles and refractory species in the initial stages of combustion, maybe due to the changing ratios of O_2 , CO_2 and CO within the burning char particles. This is supported in the literature review

[11,16,18] presented in the introductory part, where it is concluded that the gas environment, namely the relative O_2/CO_2 ratio in the oxidant mixture or the CO/CO_2 ratio in the char, affects the local char combustion temperature, the local heat transfer conditions and therefore the vaporization of elements, volatile or refractory. As indicated in [18], the increasing CO_2 in the bulk gas changes the CO/CO_2 ratio in the char particle, which could affect the vaporization of refractory oxides from the fuel char, and consequently impacts the formation of fine ash particles. This may explain the higher concentration of SiO_2 or Al_2O_3 in the finer oxyfuel ash.

From our experiments we conclude that oxyfuel combustion, as compared to air combustion, does not seem to affect the ash chemistry or the general mechanisms of ash formation, as for example, the degree of condensation or fragmentation. However, local temperature variations or the relative local $CO/CO_2/O_2$ ratios can affect the release of inorganic volatile or refractory elements, and affect therefore the composition of the fine ash material. The overall deposition behavior is not affected by this different elements release between air and oxyfuel conditions, but basically just by the different flow fields and flue gas composition in the furnace between air and oxyfuel. More focused work is required on the initial elements release under various combustion environments, as well as on their fate during the combustion process in order to get a clear conclusion on the factors affecting fine ash composition and possible links to the different ash deposition behavior.

3.6. Chemical equilibrium calculations

In order to assist the interpretation of the experimental results, chemical equilibrium calculations were performed using the equilibrium module and the integrated database of the computer program FACTSage[®] 5.5. This software calculates the concentrations of chemical species when specified elements or compounds react or partially react to reach a state of chemical equilibrium. The calculations are performed by minimization of the Gibbs free energy from the system subjected to mass balance constraints. This approach provides a first useful description of ash reactions in complex systems. However, it assumes infinitely fast reactions and therefore, it is not sufficient to describe transient processes. The compounds and phases predicted in these calculations are the more stable products (thermodynamically controlled products) and kinetic limitations are not taken into account. Moreover, the temperature history of the fuel particles during the combustion process is not taken into account and the calculations of the final product at each temperature are done independently, considering the average elemental fuel composition as the reactants and assuming perfect mixing. Therefore it has to be noted that differences in the ash formation under air or oxy conditions due to the above mentioned differences in the process are not reflected in the products predicted by chemical equilibrium calculations.

The reactants are introduced as elements, obtained from the ultimate (C, S, O, H, and N) and the elemental analysis of the fuel (Al, Ca, Fe, K, Mg, Na, P, Si and Cl), in grams contained in 1 kg of dry fuel. The trace elements have not been included in these calculations. The oxidant input corresponding to an air ratio 1.2 is also included in the reactants, being O_2 and N_2 (with a mixing ratio equal to that in air, i.e. 21 vol.% of O_2) for the air combustion and O_2 and CO_2 for the oxyfuel combustion (with a mixing ratio of 30 vol.% of O_2).

The calculations are performed for a temperature range between 800 and 1800 °C and atmospheric pressure. The possible products selected are the entire compound species (ideal gases, pure solids and pure liquids) from the ELEM, FToxid, FTsalt and FACT53 databases and the solutions species selected are listed in Table 3. When the same compound is included in more than one

Table 3
Solution species included in the Factsage calculations.

Database	Phase (full name)	Phases ^a
<i>Liquid solutions</i>		
FToxid	SLAGB (BSlag-liq)	2
FTsalt	SALTF (FSalt-liquid)	3
<i>Solid solutions</i>		
FToxid	SPIN (Spinel)	2
	MeO_A (AMonoxide)	1
	cPyr (Clinopyroxene)	1
	oPyr (Orthopyroxene)	1
	pPyr (Protopyroxene)	1
	LcPy (LowClinopyroxene)	1
	WOLLA (AWollastonite)	1
	aC2SAAa (Ca ₂ SiO ₄)	1
	Mel_ (Melilite)	1
	Oliv (Olivine)	2
	Cord (Cordierite)	1
	CORU (Corundum)	2
	NCOS (Na ₄ CaSi ₃ O ₉ - Na ₂ Ca ₂ Si ₃ O ₉ solid solution)	1
FTsalt	ACL_B (BAlkCl-ss_rocksalt)	3
	ALOH (K, Rb, Cs, [Na]//OH(HT))	1
	AOH_ (KOH-RbOH-[NaOH](LT))	1
	KCO_ (K,Na//CO ₃ ,SO ₄ (ss))	2
	KCOH (KCl-KOH(ss))	1
	KNSO (K ₃ Na(SO ₄) ₂)	1
	KSO_ (K,Na//SO ₄ ,CO ₃ (ss))	2
	NCOA (NaOH-[NaCl](ss))	1
	NCOB (NaCl-[NaOH](ss))	1
	NKCA (Na ₂ CO ₃ -[K ₂ CO ₃](LT))	1
	NKCB (Na ₂ SO ₄ [K ₂ SO ₄](ss))	1
	NKSO (Na ₂ SO ₄ [K ₂ SO ₄](ss))	1
	SCSO (K, [Ca]//CO ₃ ,SO ₄ (ss))	2
	SSUL (Na, ₄ [Mg,Ca]//SO ₄ (ss))	1

^a 1: single phase; 2: possible 2-phase immiscibility; 3: possible 3-phase immiscibility.

database, only those compounds from one database have been selected with attention to the priority list: ELEM, FToxid, FTsalt and FACT53. The slag model chosen in the FACTSage[®] calculations was the BSlag liquid. This model includes oxide components (oxides of Al, Si, Fe, Mg, Ca, Na and K) in solutions with SO₄. FACTSage[®] has, among other slag models, the slag model FToxid SLAG?, which

allows to include the oxides and all non oxide components (F, Cl, S, SO₄, PO₄, CO₃, OH/H₂O) melting together in the slag phase. However, due to its complexity, the use of this model is not encouraged, as it is not optimised for many solutions and the selection of input must be very specific. Models ASlag liquid and CSlag liquid have also been tried, but the differences found were minor, apart from the fact that their databases are not as suitable for the present chemical system.

In the following paragraphs, the presentation of the equilibrium results is directly linked to the chemical analysis results and the observations on the deposition behavior presented in the previous paragraphs.

Fig. 8 shows the maximum slag and solid ash formed for 1000 gr of dry fuel input, according to chemical equilibrium calculation results, for the combustion of the two coals in O₂/CO₂ and air and their blends with Cocoa (20 wt.%). The results seem almost identical for air and oxyfuel. Higher amounts of slag and solid phases are predicted for the pure coals compared to their blends with cocoa. The higher amounts of solid phase predicted in the pure fuels' cases are in line with the observed ash deposition behavior, where a somewhat higher deposition behavior was observed for the pure fuels' test cases. The increased input of Cl in the blend through cocoa most probably contributes to elements volatilization, reducing their tendency to form solid compounds that deposit. Other researchers have reported the formation of simple alkali salts (KCl, K₂CO₃, Na₂SO₄ and K₂SO₄) in the melted phase of biomass ashes [31,32] for fluidized bed combustors. In our case, no salt liquid solution (KCl, K₂CO₃, Na₂SO₄ and K₂SO₄)_(liq) has been obtained for the considered chemical system, which is in line with the SEM/EDS observations and ICP results of the deposit samples that did not show S and Cl in the deposited and filter ash. The oxides in the slag solution are the same predicted in the solid phase. The total sum of the amounts of the solid and the slag phase are constant, and what is changing is their relative percentage while temperature increases.

As mentioned, the ash samples collected in the deposition probes at the end of the experiments were loose and powdery. Nevertheless, during the combustion process the fuel particles are exposed to temperatures reaching the melting point of some of the ash forming compounds. In addition, vaporization and

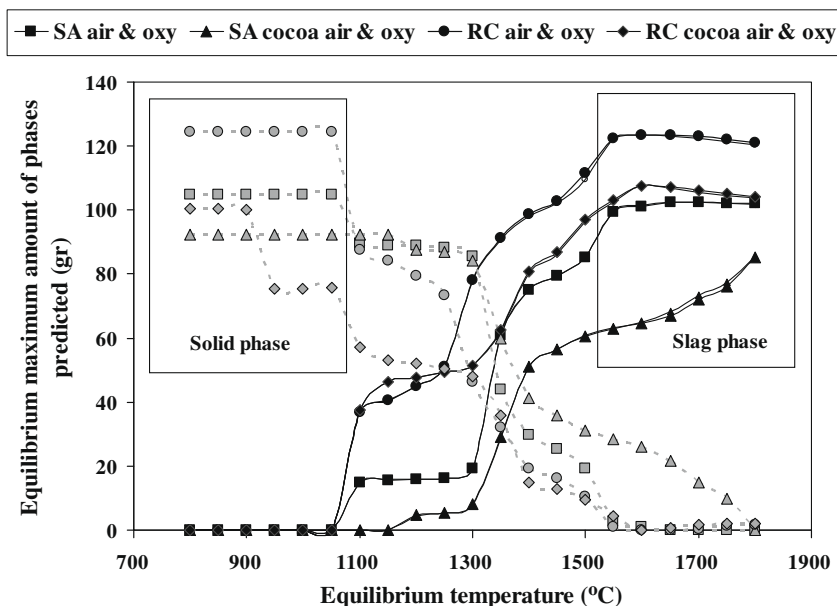


Fig. 8. Equilibrium amount (in gr/1000 gr dry fuel) of the slag and solid phase predicted by FactSage[®] versus temperature for the two coals and their blends under air and oxyfuel combustion conditions.

condensation of these compounds can occur. The rounded shape of some particles observed in the microscope supports the argument of particles' softening, not leading to slag formation though, as predicted by FACTSage[®]. Predictions on chemical equilibrium of solid compounds based on FACTSage[®] should be evaluated considering a number of parameters that affect ash formation mechanisms and slag formation but are not considered by the specific software, as for example the coal rank, fuel mineral matter composition, the initial particle size distribution of the fuel, agglomeration of ash particles with melted ash, the slag film build up on heat transfer surfaces, the particles residence time, the type of combustion system (air staging or not), heating rate of the particles.

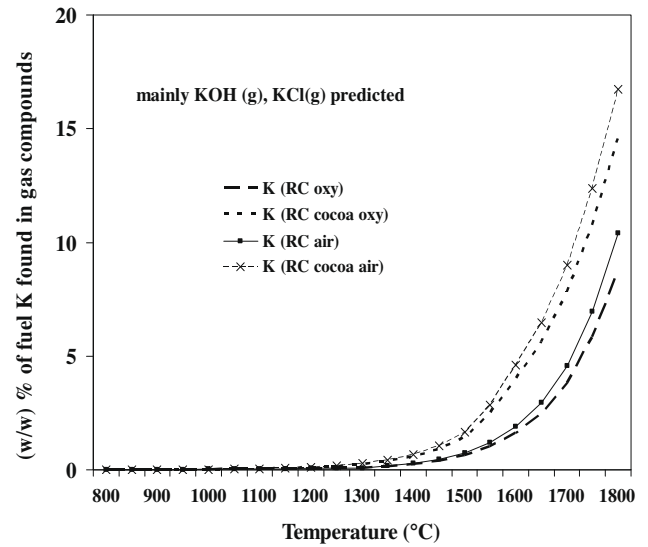
In specific, special attention must be paid when analyzing FACTSage[®] quantitative estimations of the amount of slag formed, especially concerning the potassium. The calculations do not take into account the reactivity of potassium, which varies considerably between coals and biomass fuels. The K bound in coal ash is more inert (forming aluminosilicates), than the K found in the biomass ash, which is generally not bound in silicates. The reactivity of K affects the dominating K compounds finally formed and therefore when K₂O is present in the slag model the results are much less precise.

Among the generally accepted as volatile inorganic elements (S, K, Cl), that affect the ash formation and deposition behavior, K was chosen to be studied in more detail, as S and Cl are predicted to convert into the gaseous compounds up to 100%. Fig. 9 shows the percentage of fuel K found in the gas phase for all the fuels and blends. The following discussion includes comments on the fate of K, S and Cl.

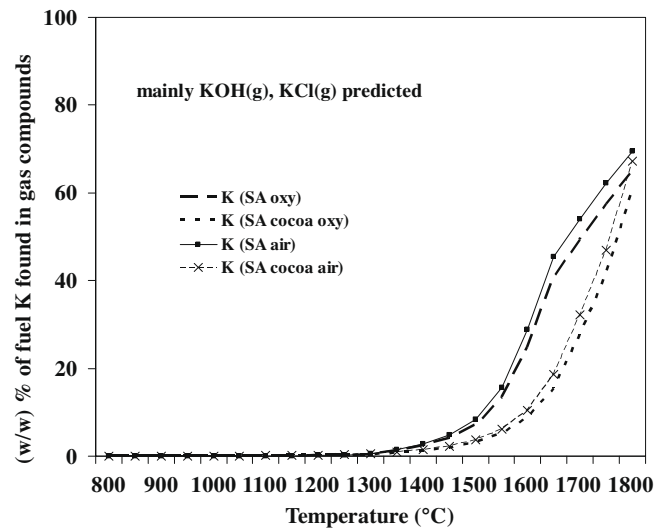
The major percentage of the fuel K forms potassium aluminum silicate (solid phase) or is found in the slag phase in the form of oxides, according to FACTSage[®] calculations. For the unblended coals in air and oxyfuel the major part of the Cl forms HCl, which unlike alkali chlorides does not condense and therefore Cl is not expected in the deposit, as verified during the ash analyses. The gaseous percentage of K is small both for the unblended coal and the blend case due to the fact that most of the alkalis are bound in aluminum silicates forming KAlSi₂O₆, NaAlSi₃O₈ and KAlSi₃O₈ (leucite and feldspars). This explains the presence of K in the deposited ash as well as in the fine ash. Aho and Ferrer [33] suggested that this mechanism in the co-firing of coal and biomass prevents chlorine deposition. Similar chemical equilibrium results were obtained by Wei et al. [34] for the co-combustion of coal and straw.

In detail, for the Russian coal in air and oxyfuel, fuel K in the gas phase is found mainly as KOH and to a lesser extent KCl_(g), under both conditions. For Cl the tendency is to form HCl_(g), and at higher temperatures some KCl_(g) starts to appear, with a maximum mass concentration of 15%. The KCl_(g) released is slightly higher under air combustion, what is in accordance with the higher K enrichment in the submicron particle range observed in the experiments. These two compounds together constitute almost 100% of the Cl species, all in the gas phase, with some elemental Cl formation predicted as well. S is all released to the gas phase, converted mainly to SO₂, and to a lesser extent to SO₃. At high temperatures, almost no SO₃ is found, and SO₂ is the thermodynamically favourable compound.

For the Russian coal/cocoa blends under both air and oxyfuel, the trend is the same for the fuel K distribution. Elemental K is also found, as well as a small percentage of K₂SO_{4(g)}. S and Cl are released in the gas phase up to 100%. HCl is formed in percentages ranging from 100% for the low temperatures down to ~20% at very high temperatures, while KCl_(g) follows the opposite trend, starting at 0% and reaching ~25% of the fuel K converted into KCl_(g). For S the trend is also the same as previously described, mostly SO₂ is formed, especially at high temperatures, while at low tempera-



(a) Russian Coal & blends



(b) South African Coal & blends

Fig. 9. Weight percentage (% w/w) of the fuel-K found in gas compounds calculated with FactSage[®].

tures a small percentage of fuel S to SO₃ was predicted as well. However, due to the Ca present in the ash, some CaSO₄ is predicted as a solid phase.

For the South African coal under oxyfuel and air, K shows the same trend as in the Russian coal case. The tendency is the same for Cl and S as well. In the South African/cocoa blends under oxyfuel and air combustion, again the same tendency was observed as in the Russian coal blend with cocoa, for K, Cl and S.

Commenting on the tendencies of these elements shown in Figs. 8 and 9, and their link with the experimental results, it is suggested that the K findings are generally in line with the experimental data. K is found back mostly in the deposited and filter ash, as the enrichment factor reveals ($EF = 1$) while S and Cl are almost completely absent from the ash. The small KCl_(g) amount predicted by the equilibrium calculations is expected to condense forming submicron particles, as observed in the cascade impactor experiments that showed Na, K and Cl enrichment in the finer ash.

Comparing the results for the coals and coal/cocoa blends, it can be remarked that a higher amount of gaseous compounds was re-

leased in the case of the blends. The reason is probably the Cl content of the ash, which is higher in the blends and facilitates the volatilization of elements, especially K. Furthermore, in the case of South African coal and its blends the gaseous release is even higher. In that case, this could be attributed to the generally higher Cl/K ratio that contributes to a larger extent to the volatilization of the available K (Table 1). A last comment is that the somewhat different flame temperatures during air and oxy combustion do not justify a large variation in the predicted solid/slag/gas phases.

4. Conclusions

Ash deposition experiments of coal and coal biomass blends were carried out in a drop tube furnace under air (O_2/N_2) and oxy fuel (O_2/CO_2) conditions. The deposition ratio and propensity were systematically higher under oxyfuel conditions; the blends have shown a lower deposition tendency than the unblended coals. The interpretation of the observed increased deposit formation under oxyfuel conditions lead to the conclusion that the different combustion conditions affect the physical properties of the flue gas and the gas flow field, causing the observed differences of deposition behavior. Unburnt carbon in ash was not observed, that would increase the deposit artificially and the ashes collected in the deposits were loose and powdery for all the experiments.

The ash analysis did not reveal changes in the ash chemistry in the oxyfuel case compared to the air case. The blending of coals with biomass in both combustion conditions is reflected in the ash chemistry, but independent of the combustion conditions, affecting the subsequent sintering tendency. A slight depletion of K could be observed in the deposited ash for the blends, probably due to the higher reactivity of biomass K and the addition of increased Cl input due to the cocoa. Almost complete absence of Cl and S was observed in the deposited ash.

A more detailed analysis of the fine ash using a cascade impactor finally implies some effect of the oxyfuel conditions compared to the air case, apart from the effect of the biomass addition. In both combustion conditions, the percentage of the elements S, P, K, Na and Ca in the submicron area of these elements is increased in relation to their percentage in the larger particle size area, probably due to condensation of volatiles on ash particles or nucleation phenomena. In the oxyfuel case the *EF* values of the refractory elements seem slightly higher than in the air case, while the volatile elements show the opposite trend. This could be explained by the effect of local char temperatures, which can be higher in the oxyfuel case, as well as the varying CO_2/CO ratio in the char combustion area, which affects the release of refractory vs. volatile elements, as suggested in the available literature. This issue however must be studied in detail in order to establish some safe conclusions and clarify the relevant mechanisms linked to the observed tendencies.

Finally, thermochemical equilibrium calculations using FACT Sage[®] show similar phase distribution and tendencies for the most important inorganic elements for slag/gas phase formation (K, Cl, S) under O_2/CO_2 and air (O_2/N_2) conditions, for the coals and their blends. It was observed that a higher amount of gaseous compounds was released in the case of the blends, probably due to the Cl content, which facilitates the volatilization of elements, especially K. The high percentage of Si rich coal ash though causes mainly formation of alkali silicates, which is the expected form of K. Furthermore the temperature at which potassium starts to be present in the slag is the same in both conditions but the percentage of the slag as well as the solid phases are higher for the unblended coals. The lower deposition propensity shown by the coal/cacao blends in the experiments, explained by the higher volatilization of the inorganic ash elements in the blend, is therefore reflected in the calculations.

Acknowledgements

The research work reported in this paper was partly carried out with the financial support from the RFCS contract number RFCR CT 2006 00010. The very fine work done by Peter Heere in carrying out the experiments is highly acknowledged.

References

- [1] Herzog HJ, Drake EM. Carbon dioxide recovery and disposal from large energy systems. *Ann Rev Energy Environ* 1996;21:145–66.
- [2] Jordal K, Anheden M, Yan J, Strömberg L. Oxyfuel combustion for coal-fired power generation with CO_2 capture – opportunities and challenges. *Greenhouse Gas Control Technol* 2005;7:201–9.
- [3] Andersson K, Johnsson F. Process evaluation of an 865MWe lignite-fired O_2/CO_2 power plant. *Energy Convers Manage* 2006;47:3487–98.
- [4] Buhre BJP, Elliott LK, Sheng CD, Gupta RP, Wall TF. Oxy-fuel combustion technology for coal-fired power generation. *Prog Energy Combust Sci* 2005;31:283–307.
- [5] Tan Y, Croiset E, Douglas MA, Thambimuthu KV. Combustion characteristics of coal in a mixture of oxygen and recycled flue gas. *Fuel* 2006;85:507–12.
- [6] Gibbins J, Chalmers H. Carbon capture and storage. *Energy Policy* 2008;36:4322–71.
- [7] Wall TF. Combustion processes for carbon capture. *Proc Combust Inst* 2007;31:31–47.
- [8] EU Demonstration Programme for CO_2 Capture and Storage (CCS), European Technology Platform for Zero Emission Fossil Fuel Power Plants (ZEP). <<http://www.zero-emissionplatform.eu/website/library/index.html#etpzeppublications>>.
- [9] Wall T, Liu Y, Spero C, Elliott L, Khare S, Rathnam R, et al. An overview on oxyfuel coal combustion—State of the art research and technology development. *Chem Eng Res Des* 2009;87:1003–16.
- [10] Sheng C, Li Y, Liu X, Yao H, Xu M. Ash particle formation during O_2/CO_2 combustion of pulverized coals. *Fuel Process Technol* 2007;88:1021–8.
- [11] Sheng C, Lu Y, Gao X, Yao H. Fine ash formation during pulverized coal combustion – A comparison of O_2/CO_2 combustion versus air combustion. *Energy Fuels* 2007;21:435–40.
- [12] Sheng C, Li Y. Experimental study of ash formation during pulverized coal combustion in O_2/CO_2 mixtures. *Fuel* 2008;87:1297–305.
- [13] Suriyawong A, Gamble M, Lee M-H, Axelbaum R, Biswas P. Submicrometer particle formation and mercury speciation under oxygen-carbon dioxide coal combustion. *Energy Fuels* 2006;20:2357–63.
- [14] Theis M, Skrifvars BJ, Zevenhoven M, Hupa M, Tran H. Fouling tendency of ash resulting from burning mixtures of biofuels. Part 2: Deposit chemistry. *Fuel* 2006;85:1992–2001.
- [15] Nelson PF. Trace metal emissions in fine particles from coal combustion. *Energy Fuels* 2007;21:477–84.
- [16] Bejarano P, Leventis YA. Single-coal-particle combustion in O_2/N_2 and O_2/CO_2 environments. *Combust Flame* 2008;153:270–87.
- [17] Murphy JJ, Shaddix RCR. Combustion kinetics of coal chars in oxygen-enriched environments. *Combust Flame* 2006;144:710–29.
- [18] Krishnamoorthy G, Veranth JM. Computational modeling of CO/CO_2 ratio inside single char particles during pulverized coal combustion. *Energy Fuels* 2003;17:1367–71.
- [19] McLennan AR, Bryant GW, Stanmore BR, Wall TF. Ash formation mechanisms during PF combustion in reducing conditions. *Energy Fuels* 2000;14:150–9.
- [20] Zheng L, Furinsky E. Assessment of coal combustion in O_2/CO_2 by equilibrium calculations. *Fuel Process Technol* 2003;81:23–34.
- [21] Zhao Y, Zhang J, Liu H, Tian J, Li Y, Zheng C. Thermodynamic equilibrium study of mineral elements evaporation in O_2/CO_2 recycle combustion. *J Fuel Chem Technol* 2006;34:641–9.
- [22] Otsuka N. A thermodynamic approach on vapor-condensation of corrosive salts from flue gas boiler tubes in waste incinerators. *Corros Sci* 2008;50:1627–36.
- [23] Jiménez S, Ballester J. Influence of operating conditions and the role of sulfur in the formation of aerosols from biomass combustion. *Combust Flame* 2005;4:346–58.
- [24] Arias B, Pevida C, Rubiera F, Pis JJ. Effect of biomass blending on coal ignition and burnout during oxyfuel combustion. *Fuel* 2008;87:2753–9.
- [25] Baxter LL. Ash deposition during biomass and coal combustion: a mechanistic approach. *Biomass Bioenergy* 1993;4:85–102.
- [26] Nielsen HP, Baxter LL, Sclippa G, Morey C, Frandsen FJ, Dam-Johansen K. Deposition of potassium salts on heat transfer surfaces in straw-fired boilers: a pilot-scale study. *Fuel* 2000;79:131–9.
- [27] Robinson AL, Junker H, Baxter LL. Pilot-scale investigation of the influence of coal-biomass cofiring on ash deposition. *Energy Fuels* 2002;16:343–55.
- [28] Miettinen Westberg H, Bystroem M, Leckner B. Distribution of potassium, chlorine, and sulfur between solid and vapor phases during combustion of wood chips and coal. *Energy Fuels* 2003;17:18–28.
- [29] Andersen KH, Frandsen FJ, Hansen PFB, Wieck-Hansen K, Rasmussen I, Overgaard P, et al. Deposit formation in a 150 MW_e utility pf-boiler during co-combustion of coal and straw. *Energy Fuels* 2000;14:765–80.

- [30] Buhre BJP, Hinkley JT, Gupta RP, Wall TF, Nelson PF. Submicron ash formation from coal combustion. *Fuel* 2005;84:1206–14.
- [31] Skrifvars BJ, Backman R, Hupa M. Characterization of the sintering tendency of ten biomass ashes in FBC conditions by a laboratory test and by phase equilibrium calculations. *Fuel Process Technol* 1998;56:55–67.
- [32] Zevenhoven-Onderwater M, Backman R, Skrifvars BK, Hupa M. The ash chemistry in fluidized bed gasification of biomass fuels. Part I: Predicting the chemistry of melting ashes and ash-bed material interaction. *Fuel* 2001;80:1489–502.
- [33] Aho M, Ferrer E. Importance of coal ash composition in protecting the boiler against chlorine deposition during combustion of chlorine-rich biomass. *Fuel* 2005;84:201–12.
- [34] Wei X, Lopez C, Von Puttkamer T, Schnell U, Unterberger S, Hein KRG. Assessment of chlorine-alkali-mineral interactions during co-combustion of coal and straw. *Energy Fuels* 2002;16:1095–108.